

# Synthesis of two-species ion chains for a new optical frequency standard with an indium ion

K. Hayasaka

Received: 2 May 2011 / Revised version: 18 November 2011 / Published online: 7 February 2012  
© Springer-Verlag 2012

**Abstract** Ion chains consisting of different species play an important role in new applications in quantum information processing as well as in optical frequency standards. We demonstrate generation and stabilization of ion chains consisting of  $\text{Ca}^+$  and  $\text{In}^+$ . The  $\text{Ca}^+$  chains with  $\text{In}^+$  located at specified positions are synthesized using resonant photoionization, real-time imaging and trap field control techniques. A specific configuration of an ion chain is stabilized by destabilizing other configurations via selective excitation of vibrational modes using amplitude modulation on the cooling laser beam. New approaches to an indium ion optical clock are proposed using the ions chains.

## 1 Introduction

Cold ions trapped and laser-cooled in rf traps supply ideal quantum systems with well-defined position and virtually unlimited interaction time with optical fields [1]. This feature, realized by combination of steep trap potential and laser cooling, is exploited in many applications in quantum information processing (QIP) and in optical frequency standards. Various small-scale QIP protocols have been realized with up to 14 ions [2, 3]. Unprecedented accuracy in optical frequency measurement with a fractional uncertainty of  $10^{-18}$  level has been demonstrated in systems based on  $\text{Hg}^+$  and on  $\text{Al}^+$  [4, 5]. An important step toward further development is to overcome the anomalous motional heating arising from current fluctuations of the trap electrode surface [6],

which degrades the fidelity of quantum gate operations as well as that of detecting the quantum states after the clock laser illumination. However, once a quantum state is written to an ion, laser cooling cannot be used as a measure against the heating, because it relies on emission of photons accompanying destruction of the quantum states. One possible solution is sympathetic cooling with refrigerator ions inserted in the target ion chain [7]. In this method only the refrigerator ions are subject to cooling laser beams, and any motional energy excited in the target ions is cooled via Coulomb coupling without disturbing the quantum state of the target ions. The first essential step toward this direction is preparation of two-species ion chain [8]. We report on synthesis, stabilization and an application of the two-species ion chains consisting of  $\text{Ca}^+$  and  $\text{In}^+$ .

$^{40}\text{Ca}^+$  is one of the most popular ion species in QIP, and milestone experiments including 14-ion entanglement have been demonstrated with the ion [2, 3]. In these studies the  $^2\text{S}_{1/2}-^2\text{P}_{1/2}$  transition depicted in Fig. 1(a) (397 nm, natural linewidth 20 MHz) supplies a convenient way to cool and observe the ion.  $^{115}\text{In}^+$  has an alkaline-earth-like electron configuration and the  $^1\text{S}_0-^3\text{P}_0$  transition shown in Fig. 1(a) (237 nm, natural linewidth 0.8 Hz) was previously proposed as an optical frequency standard with an uncertainty of  $10^{-18}$  level [10], although reported measurement still remains at  $10^{-13}$  level [11, 12]. Besides the clock transition,  $\text{In}^+$  supplies a convenient transition ( $^1\text{S}_0-^3\text{P}_1$ , 230 nm, natural linewidth 360 kHz) for sideband cooling [13]. The combination of the two species is an essential step toward two applications. In the first application,  $\text{In}^+$  ions are inserted in between  $\text{Ca}^+$  ions and are continuously laser-cooled to keep the  $\text{Ca}^+$  qubits at cold temperatures [8]. This supplies an essential step toward large-scale QIP, in which the qubits have to stay in the motional ground state while waiting for the next gate operations in microtraps [9]. In the second ap-

K. Hayasaka (✉)  
National Institute of Information and Communications  
Technology, 588-2 Iwaoka, Iwaoka-cho Nishi-ku, Kobe  
651-2492, Japan  
e-mail: hayasaka@nict.go.jp

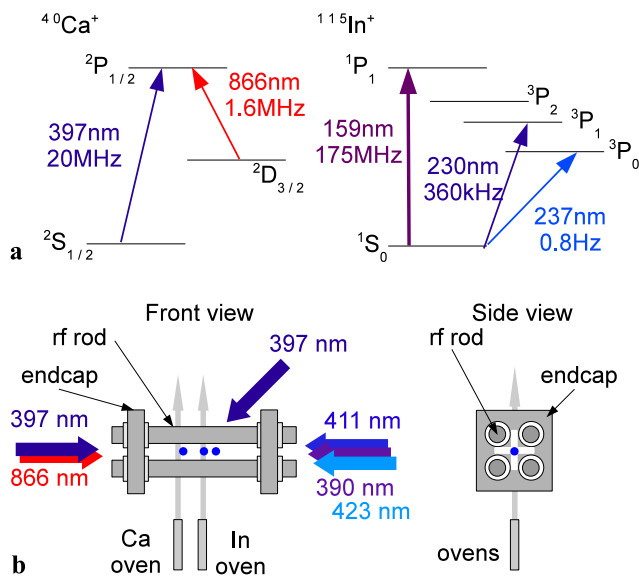


**Fig. 1** (a) Energy levels of  $^{40}\text{Ca}^+$  and  $^{115}\text{In}^+$ . Transition wavelengths and linewidths are shown. (b) Experimental setup

plication,  $\text{Ca}^+$  ions serve as the refrigerator and an  $\text{In}^+$  is used as a reference of an optical frequency standard. The quantum logic spectroscopy (QLS) uses the refrigerator ion also as the logic ion [4, 5], but its use solely for cooling would contribute to improve the performance of the  $\text{In}^+$  optical clock by supplying continuous cooling. In both applications the essential building block is an ability to generate  $\text{Ca}^+$  chains with  $\text{In}^+$  placed at specified locations. We demonstrate a simple way of synthesizing such ion chains using real-time imaging, resonant photo-ionization and trap field control techniques in a traditional linear trap. A novel method for stabilizing a specific ion configuration is demonstrated using destabilization of other configurations via selective excitation of vibrational modes by amplitude modulation on the cooling laser beam.

## 2 Experimental setup

The experimental setup is outlined in Fig. 1(b). The trap is a traditional linear trap made of stainless steel, characterized by a dimension of  $r_0 = 1.8$  mm (center to electrode distance),  $2z_0 = 10$  mm (trap length) driven at a frequency of 12.6 MHz. The rf voltage  $\pm V_0/2$  is applied to two pairs of diagonal rf rods. Two supporting plates of the four rods are insulated from the rods by ceramic spacers, and are used as the endcaps that control the axial trapping potential by DC voltages. The indium oven is located 5 mm below the trap center, while the calcium oven is placed 3 mm away from the indium oven. The vacuum part is contained in a stainless chamber and evacuated down to  $1 \times 10^{-8}$  Pa. Laboratory-made external-cavity diode lasers (ECDLs) at

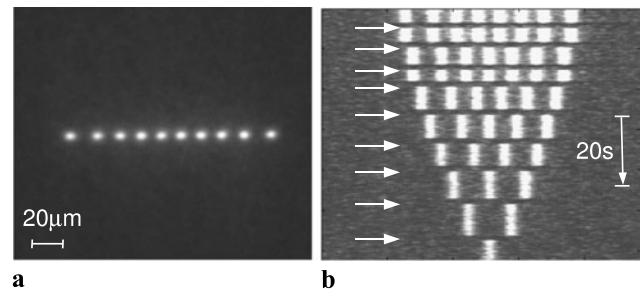


**Fig. 2** (a) Image of 10  $\text{Ca}^+$ . (b) Time evolution of the intensity profile of a  $\text{Ca}^+$  chain along axial direction during the  $\text{Ca}^+$  chain preparation. Time evolves from top to bottom. The arrows show the ‘kick-out’ operations to reduce  $\text{Ca}^+$ . In this example,  $\text{Ca}^+$  chains containing from one up to eight ions are obtained by stopping the reduction procedure at the desired number

423 and 390 nm are used for photo-ionization of calcium, while a single ECDL at 411 nm serves as the indium ionization laser. To avoid amplified spontaneous emission background from the ECDLs causing unwanted excitation to extraneous energy levels, the ECDLs at 397 and at 866 nm each incorporate a filter cavity similar to the system reported previously [14]. Fluorescence of  $\text{Ca}^+$  at 397 nm is imaged onto an image-intensified CCD (ICCD) camera via a single lens with a magnification of about 20, and real-time image is processed on a PC after averaging for 300 ms as shown in Fig. 2(a). The ion chains are monitored on the PC display using a labview-based program, which also shows the intensity profiles along trap axis. The rf and DC voltages are controlled based on the observation outcome.

## 3 Ion chain synthesis

Our ion chain synthesis consists of three steps. In the first step a chain of  $\text{Ca}^+$  is generated in a linear trap by resonant photo-ionization of a neutral calcium beam, followed by laser cooling with a 397-nm and a 866-nm diode lasers. The number of  $\text{Ca}^+$  is identified and adjusted in real time by imaging the fluorescence at 397 nm. In the second step,  $\text{In}^+$  ions are added in the  $\text{Ca}^+$  chain by resonant photo-ionization of an indium beam.  $\text{In}^+$  ions are identified as dark sites appearing in the chain. A chain consisting of specified number of  $\text{Ca}^+$  and  $\text{In}^+$  is prepared at this point, and the locations of  $\text{In}^+$  are adjusted in the final step. DC voltages applied to the trap endcaps are lowered so that  $\text{In}^+$  ions experience random hops to various locations in the chain. Upon encountering the desired location pattern the DC voltages are raised to freeze the pattern. Details of the procedure is described in the following.

A chain of  $\text{Ca}^+$  with a specified number is prepared in the first step. With illumination of the cooling and photo-ionization laser beams the calcium oven is heated for 60 seconds to load  $\text{Ca}^+$  to the trap. The trapping secular frequency

is set to  $w_r/(2\pi) = 830$  kHz and  $w_z/(2\pi) = 110$  kHz for radial and for axial directions, respectively. Ion chains with more than 10  $\text{Ca}^+$  are obtained, but the number depends on such parameters as laser power and detuning, and was not constant in the present setup. A period of lower rf voltages for one second, which we call ‘kick-out’ pulse, is applied to the rf electrodes repeatedly to remove the ions one by one until the desired number is reached. With an appropriate value of the low rf voltage, the reduction process worked with high probability and reproducibility as shown in Fig. 2(b). The secular frequency of the low voltage period was  $w_r/(2\pi) = 103$  kHz in the experiment. We also tried one-by-one loading strategy, but it was not successful due to excess  $\text{Ca}^+$  ions appearing even after the oven is turned off, presumably because of slow rate of initial cooling.

In the next step, indium ions are loaded to the  $\text{Ca}^+$  chain by resonant photo-ionization. The ionization process is actually a two-step excitation, but both transitions are excited with a single 411-nm laser with a power of 2 mW due to coincidence of the two wavelengths [15]. The indium oven was heated while the ionization laser illuminated the trap center. A bandpass interference filter centered at 397 nm was placed in front of the ICCD camera to block scattering at 411 nm and to observe the  $\text{Ca}^+$  chain continuously. Time evolution of the 397-nm fluorescence profile along the trap axis is shown in Fig. 3(a), in which we tried to insert one  $\text{In}^+$  to a four- $\text{Ca}^+$  chain.  $\text{In}^+$  is identified as dark sites appearing in the chain. This diagnosis method is valid as long as the ions keep the crystallized state. Occasional melt of the chain into a cloud state is shown in Fig. 3(a) as long dark periods indicated by dashed arrow. In the cloud state  $\text{Ca}^+$  are not visible anymore due to Doppler broadening. The ion cloud is brought back to the chain by inserting a period of lower rf voltage to reduce rf-heating. No  $\text{Ca}^+$  was lost during the loading process. Although individual  $\text{In}^+$  is identified, due to slow speed of initial sympathetic cooling excess  $\text{In}^+$  ions appeared to the chain even after the oven current was turned off. The excess  $\text{In}^+$  ions were discarded again in the same way as in the first step to remove the excess  $\text{Ca}^+$ . In this step, the lower voltage of the kick-out was set so that only  $\text{In}^+$  is swept out from the trap. The voltage can be chosen in this way, because the radial secular frequency is inversely proportional to ion mass, and  $\text{In}^+$  feels  $40/115 \sim 0.35$  of the trapping frequency of  $\text{Ca}^+$ . This procedure is also shown in Fig. 3(a), in which two excess  $\text{In}^+$  were removed and only one  $\text{In}^+$  was kept in the chain.

In the final step the desired configuration of  $\text{Ca}^+$  and  $\text{In}^+$  is obtained by randomizing it deliberately first and then by freezing it upon finding the proper pattern. The hopping rate of  $\text{In}^+$  in the chain can be controlled by the DC voltages applied to the endcaps. The hop is completely forbidden with high voltages, whereas the rapid hops that cannot be captured in one imaging frame occur with too low voltages. The

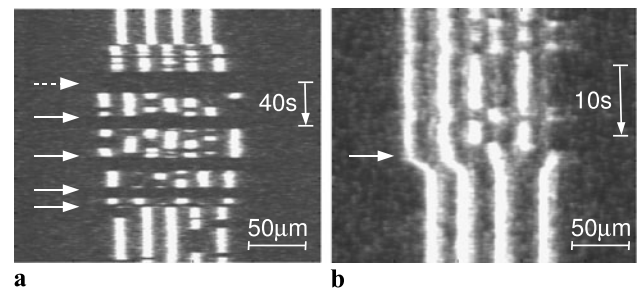


**Fig. 3** (a) Procedure of inserting one  $\text{In}^+$  to a four- $\text{Ca}^+$  chain.  $\text{In}^+$  are identified as hopping dark sites. Three  $\text{In}^+$  ions were added first, but were removed one by one until one  $\text{In}^+$  is present. The dashed arrow denotes melt of the chain, while the solid arrows represent the moments when the kick-out pulses are applied. (b) Procedure of randomizing and of fixing the  $\text{In}^+$  locations. The arrow indicates the instant when the DC voltages are increased. The final ion pattern is ( $\text{Ca}^+$ ,  $\text{Ca}^+$ ,  $\text{In}^+$ ,  $\text{Ca}^+$ ,  $\text{In}^+$ )

rate of the rapid hops is larger than 3 Hz estimating from the integration period of the imager. We assume the change in the confinement along the axial direction is responsible for the change in the hopping rate. With appropriate intermediate voltages the patterns of  $\text{Ca}^+$ – $\text{In}^+$  arrangement change frequently but each pattern stays for several imaging frames. This enables adiabatic raise of the DC voltages to freeze the pattern upon observing the desired pattern in the fluorescence profile. This randomizing and freezing technique is shown in Fig. 3(b). In this example, the DC voltages were raised from 10 to 22 V with 0.1 V step in 1 second to fix the pattern as ( $\text{Ca}^+$ ,  $\text{Ca}^+$ ,  $\text{In}^+$ ,  $\text{Ca}^+$ ,  $\text{In}^+$ ).

Distances between the neighboring ions in the chain do not depend on the ion species as long as they are singly charged [8]. This fact leaves a possibility that our dark ions might be some ions other than  $\text{In}^+$ , for example, those ionized from residual gas. This possibility is easily excluded by the fact that the dark sites are observed only in the presence of both the neutral indium atomic beam and the 411-nm ionizing laser. As an additional diagnosis of the dark ions without using a resonant light source for  $\text{In}^+$ , we demonstrate frequency measurement of vibrational modes of two-species chain. The mode frequency of the chain along axial direction depends on the mass as well as the arrangement of the ions, and can be calculated numerically [8]. For an ion chain consisting of two  $\text{Ca}^+$  and two  $\text{In}^+$  the lowest frequencies are calculated as 0.689, 0.702 and 0.703 relative to that of two- $\text{Ca}^+$  center-of-mass mode. Experimentally the modes are excited by rf voltage applied to one of the endcaps, and the resonance is observed as enhanced amplitude of  $\text{Ca}^+$  motion along the trap axis. Figure 4 shows this measurement. For the trapping voltage corresponding to center-of-mass mode frequency of 110.8 kHz of  $\text{Ca}^+$  in Fig. 4(a), the frequencies calculated for the chain with two  $\text{Ca}^+$  and two  $\text{In}^+$  are located in between 76.3 and 77.9 kHz. The measurement shown in Fig. 4(b) is in good agreement with this calculation, and this verifies the dark sites as  $\text{In}^+$ .

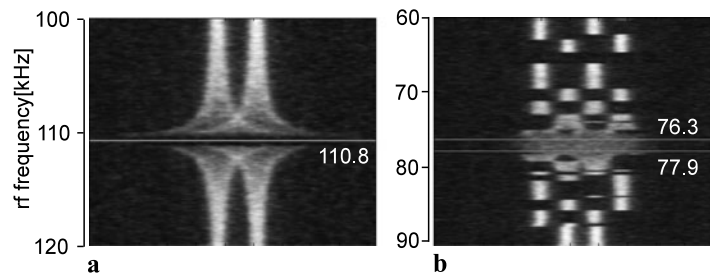


**Fig. 4** (a) Mode frequency measurement of two  $\text{Ca}^+$ . Frequency is scanned from 100 to 120 kHz and the resonance is found at 110.8 kHz marked with the horizontal line. (b) The measurement with two  $\text{Ca}^+$

and two  $\text{In}^+$ . Frequency is scan from 60 to 90 kHz. The resonance is observed as a band in between 76.3 and 77.9 kHz, both marked with solid lines

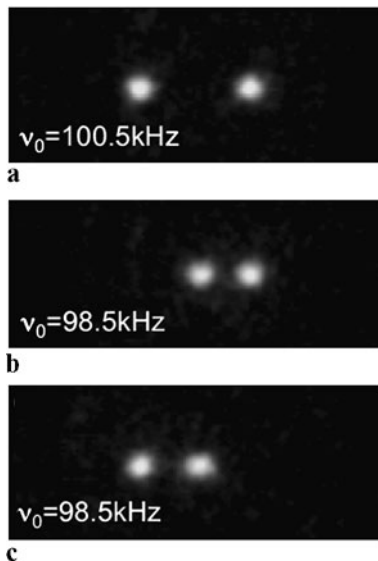


**Fig. 5** Configurations of one  $\text{In}^+$  and two  $\text{Ca}^+$ .  $\text{In}^+$  is indicated by the dark site. (a) ( $\text{Ca}^+$ ,  $\text{In}^+$ ,  $\text{Ca}^+$ ). (b) ( $\text{In}^+$ ,  $\text{Ca}^+$ ,  $\text{Ca}^+$ ). (c) ( $\text{Ca}^+$ ,  $\text{Ca}^+$ ,  $\text{In}^+$ ). The frequencies of the lowest vibrational mode are shown in each configuration

#### 4 Stabilization of ion configuration

Although the basic method for generating the  $\text{In}^+$ - $\text{Ca}^+$  chains is demonstrated in the previous section, the configurations have to be kept stable for a long period in real applications. A simple method for stabilizing a specific configuration is discussed in this section. A chain consisting of one  $\text{In}^+$  located at the middle of two  $\text{Ca}^+$  obtained in the way described in the previous sections is shown in Fig. 5(a). This configuration is ideal for further measurement and manipulation of the  $\text{In}^+$ , but this target changes into unwanted ones shown in Figs. 5(b), (c) after seconds. The time evolution of the intensity distribution along the horizontal axis is shown in Fig. 6(a), which indicates that the target configuration occupies only a small fraction of time. The transition might be due to momentum kick by spontaneous emission, or by collision with background gas, but complete suppression of the transition was not viable.

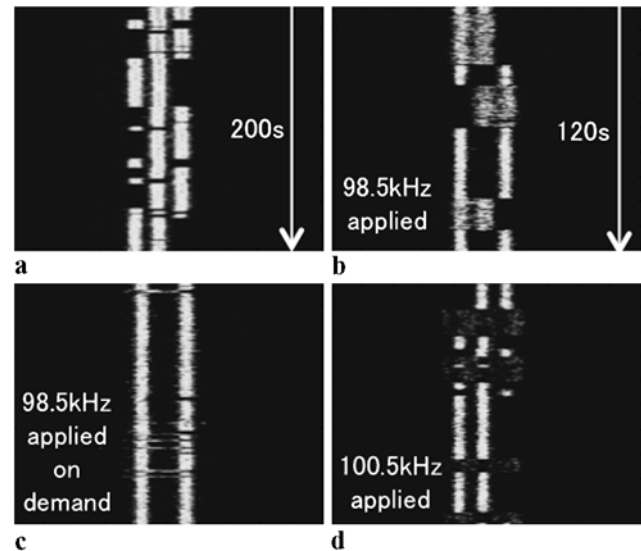


**Fig. 6** Time evolution the  $\text{In}^+$ - $\text{Ca}^+$  chain. (a) The transition occurs frequently without applying amplitude modulation to the 397-nm laser. (b) The unwanted configurations are immediately destabilized by impinging the amplitude modulation at 98.5 kHz to the cooling laser upon they are found. (c) Only the unwanted configurations are destabilized with 98.5-kHz excitation. (d) The target configuration is destabilized at 100.5-kHz excitation

A novel method for stabilizing the target is implemented by exciting vibration of the unwanted configurations. The frequency of the lowest mode along the trap axis depends on the configuration, and is calculated numerically as shown in Figs. 5(a)–(c) [8]. Although the frequency difference is small, selective excitation is easily realized by adding amplitude modulation to the 397-nm laser beam. Figure 6(c) shows that only the configurations (b) and (c) are disturbed when the resonant frequency is applied. This should be contrasted to the opposite case shown in Fig. 6(d). By optimizing the modulation parameters, fast destabilization of the unwanted configurations can be realized. Manual switching of the modulation upon encountering the unwanted configuration keeps the target during the most of the period as shown in Fig. 6(b), which would be automated easily.



The frequency difference of the vibrational frequencies of different configurations becomes smaller with decreasing mass ratio, and this limits application of the destabilization method. Larger frequency difference of higher modes [8] might be useful in extending the applicable mass ratio range. In the optical clock application described in the next section, the stabilization periods can be inserted before and after the clock laser illumination. In quantum information applications the stabilization method cannot prevent ions from switching positions during quantum gate operations but it is useful in preparing the same initial ion configurations repeatedly.

## 5 Optical clock with a sympathetically-cooled indium ion

The ion chains prepared in our method provide a platform for a new optical frequency standard with  $\text{In}^+$ . The original proposal with a single ion optical clock with an alkaline-earth-metal-like electron structure was made already in 1982 [10], but the predicted uncertainty in the order of  $10^{-18}$  has not been achieved until recently due to difficulty in cooling and observing the ion with vacuum ultraviolet (VUV) radiation. The issue has been solved by employing quantum logic spectroscopy (QLS) which eliminates the need for the VUV radiation. The unprecedented fractional uncertainty of  $8.6 \times 10^{-18}$  was reported with  $^{27}\text{Al}^+$  using QLS [5]. Another promising candidate for an inaccuracy of  $10^{-18}$  is indium ion ( $^{115}\text{In}^+$ ), whose blackbody radiation shift is estimated be smaller than those of other neutral and ionic clock candidates except  $\text{Al}^+$  [16].

Energy levels and transitions of the  $\text{In}^+$  ion are shown in Fig. 1(a). The original idea of the  $\text{In}^+$  single-ion clock assumes the use of the  $^1\text{S}_0$ – $^1\text{P}_1$  transition at 159 nm for laser cooling as well as for state detection [10]. Due to the difficulty in generating the single-mode coherent radiation in the vacuum ultraviolet (VUV) region, an alternative approach to use  $^1\text{S}_0$ – $^3\text{P}_1$  (230 nm, linewidth 360 kHz) has been deployed previously [11, 12]. We propose another approach, in which an  $\text{In}^+$  in the Lamb–Dicke regime is prepared by sympathetic cooling by  $^{40}\text{Ca}^+$  as described in the previous sections. Sideband cooling of the ion chain using the  $^2\text{S}_{1/2}$ – $^2\text{D}_{5/2}$  of the  $\text{Ca}^+$  would bring the  $\text{In}^+$  to a lower temperature [17]. Diagnosis on the quantum state of the  $\text{In}^+$  after irradiation of the clock transition (236.5 nm, linewidth 0.8 Hz) is made by one of the following three methods. The first method uses QLS as in  $\text{Al}^+$  after initialization of an ion chain including a  $\text{Ca}^+$  and an  $\text{In}^+$  to the vibrational ground state of the center-of-mass motion. The QLS makes the diagnosis faster by detection of  $\text{Ca}^+$   $^2\text{S}_{1/2}$ – $^2\text{P}_{1/2}$  transition (linewidth 20 MHz) instead of the  $\text{In}^+$  transition. In the second method the  $^1\text{S}_0$ – $^1\text{P}_1$  transition (159 nm) is directly excited by 5th harmonic pulses of a 795-nm femto-second Ti:S

laser generated in xenon gas jet located at the beam waist of an enhancement cavity [18]. If sufficient power is available for the excitation, the large decay rate (1.1 GHz) of the  $^1\text{P}_1$  state reduces the diagnosis time significantly. In the third method the  $^1\text{S}_0$ – $^3\text{P}_1$  transition (230 nm) is used as in the previous studies, but our approach deploys a 237-nm clock laser stabilized to a strontium optical lattice clock via optical frequency comb to assure the frequency stability of the clock laser during the rather long diagnosis period over 100 seconds. This *hybrid optical clock* approach might provide an ultimate optical clock by combining the ultimate *stability* of the optical lattice clock and the ultimate *accuracy* of the single-ion clock. Effort to establish the new  $\text{In}^+$  optical clock by employing these three methods to the sympathetically cooled  $\text{In}^+$  is in progress at our institute.

## 6 Conclusion

In summary, we have demonstrated a simple way to prepare two-species ion chains containing  $\text{Ca}^+$  and  $\text{In}^+$  based on standard technologies of ion trapping. A novel technique for stabilizing the target ion chain has been demonstrated by destabilizing the unwanted configurations via selective excitation of configuration-dependent vibrational frequency. A new optical frequency standard based on the sympathetically-cooled indium ion has been proposed using three schemes, namely, QLS, VUV direct excitation, and hybrid clock. We emphasize that the hybrid optical clock might realize an ultimate optical clock by combining the stability of the optical lattice clock and the accuracy of the single-ion optical clock.

Besides the applications in the two research fields, our method might be useful in applications of various cold ions. Conventional laser-cooling methods exclude application to ions without cyclic optical transitions including molecular ions, but our method supplies a convenient way to prepare such ions at specified locations with  $\mu\text{m}$ -level spatial resolution at low temperatures as well as to identify them even without a resonant light source. The fact that  $^{115}\text{In}^+$  was sympathetically cooled with  $^{40}\text{Ca}^+$  down to a temperature to form a crystallized state suggests that heavier ions can be cooled efficiently even with lighter ions. Use of heavier refrigerator ions such as  $^{138}\text{Ba}^+$  and  $^{172}\text{Yb}^+$  might extend applicable mass range of our method. We note that the crucial requirement of our method is access to resonant photo-ionization.

**Acknowledgements** The author thanks T. Ido, Y. Li, K. Matsubara K. Wakui and M. Kajita for contribution to the new indium ion clock design. This work was partly supported by JST CREST funding program “Creation of New Technology Aiming for the Realization of Quantum Information Processing Systems”.

## References

1. D. Leibfried, R. Blatt, C. Monroe, D. Wineland, *Rev. Mod. Phys.* **75**, 281 (2003)
2. R. Blatt, D. Wineland, *Nature* **453**, 1008 (2008)
3. T. Monz, Ph. Schindler, J.T. Barreiro, M. Chwalla, D. Nigg, W.A. Coish, M. Harlander, W. Haensel, M. Hennrich, Rainer Blatt, *Phys. Rev. Lett.* **106**, 130506 (2011)
4. T. Rosenband, D.B. Hume, P.O. Schmidt, C.W. Chou, A. Brusch, L. Lorini, W.H. Oskay, R.E. Drullinger, T.M. Fortier, J.E. Stalnaker, S.A. Diddams, W.C. Swann, N.R. Newbury, W.M. Itano, D.J. Wineland, J.C. Bergquist, *Science* **319**, 1808 (2008)
5. C.W. Chou, D.B. Hume, J.C.J. Koelemeij, D.J. Wineland, T. Rosenband, *Phys. Rev. Lett.* **104**, 070802 (2010)
6. L. Deslauriers, S. Olmschenk, D. Stick, W.K. Hensinger, J. Sterk, C. Monroe, *Phys. Rev. Lett.* **97**, 103007 (2006)
7. D.J. Larson, J.C. Bergquist, J.J. Bollinger, W.M. Itano, D.J. Wineland, *Phys. Rev. Lett.* **57**, 70 (1986)
8. G. Morigi, H. Walther, *Eur. Phys. J. D* **13**, 261 (2001)
9. D. Kielpinski, C. Monroe, D.J. Wineland, *Nature* **417**, 709 (2002)
10. H.G. Dehmelt, *IEEE Trans. Instrum. Meas.* **IM-31**, 83 (1982)
11. J. von Zanthier, Th. Becker, M. Eichenseer, A.Yu. Nevsky, Ch. Schwedes, E. Peik, H. Walther, R. Holzwarth, J. Reichert, Th. Udem, T.W. Hänsch, P.V. Pokasov, M.N. Skvortsov, S.N. Bagayev, *Opt. Lett.* **25**, 1729 (2000)
12. Y.H. Wang, R. Dumke, T. Liu, A. Stejskal, Y.N. Zhao, J. Zhang, Z.H. Lu, L.J. Wang, Th. Becker, H. Walther, *Opt. Commun.* **273**, 526 (2007)
13. E. Peik, J. Abel, Th. Becker, J. von Zanthier, H. Walther, *Phys. Rev. A* **60**, 439 (1999)
14. J. Labaziewicz, P. Richerme, K. Brown, I. Chuang, K. Hayasaka, *Opt. Lett.* **32**, 572 (2007)
15. Y.H. Wang, R. Dumke, T. Liu, A. Stejskal, Y.N. Zhao, L. Zhang, Z.H. Lu, L.J. Wang, Th. Becker, H. Walther, *Laser Phys.* **17**, 1017 (2007)
16. T. Rosenband, W.M. Itano, P.O. Schmidt, D.B. Hume, J.C.J. Koelemeij, J.C. Bergquist, D.J. Wineland, in *Proc. 20th European Frequency and Time Forum (EFTF)*, Braunschweig (2006)
17. H. Sawamura, K. Kanda, R. Yamazaki, K. Toyoda, S. Urabe, *Appl. Phys. B* **93**, 381 (2008)
18. Ch. Gohle, Th. Udem, M. Herrmann, J. Rauschenberger, R. Holzwarth, H.A. Schuessler, F. Krausz, T.W. Hänsch, *Nature* **436**, 234 (2005)